Journal of Molecular Graphics and Modelling 27 (2008) 563–567

Contents lists available at ScienceDirect

Journal of Molecular Graphics and Modelling

journal homepage: www.elsevier.com/locate/JMGM

Short communication

In silico description of fluorescent probes *in vivo*

Sergio Pantano *

Institut Pasteur of Montevideo, Calle Mataojo 2020, CP 11400, Montevideo, Uruguay

ARTICLE INFO

Article history:
Received 30 April 2008
Received in revised form 11 August 2008
Accepted 16 August 2008
Available online 23 August 2008

Keywords:
cAMP
Rational design
Molecular dynamics
FRET
GFP
Implicit solvation
Generalized Born model

ABSTRACT

Fluorescent imaging *in vivo* has became one of the most powerful tools to follow the temporal and spatial localization of a variety of intracellular molecular events. Genetically encoded fluorescent indicators using the FRET effect are routinely used although the molecular basis regulating their functioning is not completely known. Here, the structural and dynamics properties of a commonly used FRET sensor for the second messenger cAMP based on the cAMP-binding domains of the regulatory subunit of Protein Kinase A are presented. Molecular dynamics simulations allowed pinpointing the main features of cAMP driven conformational transition and dissecting the contributions of geometric factors governing the functioning of the biosensor. Simulations suggest that, although orientational factors are not fully isotropic, they are highly dynamic making the inter-chromophore distance the dominant feature, determining the functioning of the probes. It is expected that this computer-aided methodology may state general basis for rational design strategies of fluorescent markers for *in vivo* imaging.

1. Introduction

A number of genetically encoded fluorescent sensors have been developed on the base of spectral variants of the green fluorescent protein (GFP) and the phenomenon of Förster resonance energy transfer (FRET) [1]. They constitute a unique tool to scrutinize extra and intracellular signal transduction by direct visualization of individual molecular events in real time on living cells granting novel insights on problems of biological and medical relevance [2–4].

The FRET effect consists in non-radiative, distance-dependent, transfer of energy between donor and acceptor chromophores by dipole–dipole interaction at a maximum reciprocal distance of nearly 10 nm. Thus, if a given donor is excited by incident light and an acceptor is in close proximity, part of the donor's excited state energy is transferred to the acceptor. This leads to a reduction in the donor's emission fluorescence intensity, excited lifetime and an increase in the acceptor's emission intensity [5]. Being a dipole–dipole interaction, the energy transfer varies with the relative orientation of the dipole moments of donor and acceptor, which is called the orientational factor (kappa-squared) as defined in Fig. 1, and upon a variation in their spatial separation.

Minimally, two components are needed to build up a FRET-based indicator: (i) a sensor, which may consist of two interacting proteins or a single protein domain undergoing a significant conformational transition upon changes in the environmental conditions such as the rise in the local concentration of a ligand and (ii) a donor and an acceptor chromophores (most frequently spectral variants of GFP) genetically fused to the sensor. Hence, a change in the acceptor–donor distance or reciprocal orientation due to protein binding or a conformational transition can be read as a change in the FRET signal. Owing to the relatively small number of proteins determined in both, bound and unbound states, the difficulty to follow conformational transitions by experimental means and the impossibility to reliably predict the relative orientation of the chromophores fused to the sensor the construction of FRET-based fluorescent probes is normally a trial and error process subject to an undetermined number of iterative improvements [6]. Moreover, there is no way to know a priori whether the geometry of a given sensor will allow to further improving its efficiency. Aimed to provide an alternative approach, the mechanistic description of a commonly used fluoresce sensor for the second messenger cyclic Adenosine Mono Phosphate (cAMP) is provided here on the base of molecular dynamics (MD) simulations. Within this framework, the relatively long simulation times required to properly sample conformational transitions may hamper the use of explicit solvent MD simulations. Nevertheless, the use of implicit solvent simulations may provide a valid and

* Tel.: +598 25220910x156; fax: +598 25224185.
E-mail address: spantano@pasteur.edu.uy.

1093-3263/$ – see front matter © 2008 Elsevier Inc. All rights reserved.
doi:10.1016/j.jmgm.2008.08.003

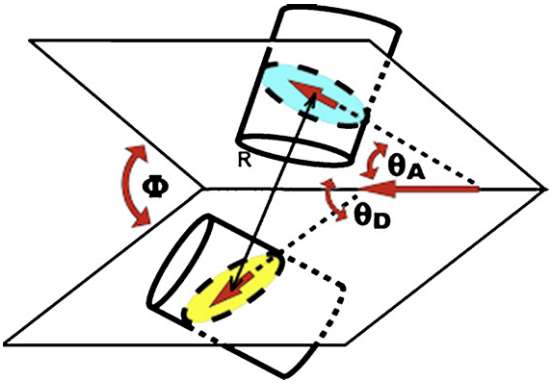

Fig. 1. Calculation of FRET efficiency. Simulated FRET was calculated from the instantaneous distances and geometrical determinants obtained from the MD simulations using the relations: $E\% = [1/(1 + R_o/R)]^6$; where $R_o = 9.78 \times 10^3 \times (Q_d\kappa^2 n^{-4} J)^{1/6}$. The orientational factor κ^2 is defined as $\kappa^2 = [\sin(\theta_D)\sin(\theta_A)\cos(\phi) - 2\cos(\theta_D)\cos(\theta_A)]^2$, where n is the refractive index, Q_d is the quantum yield and J the overlap integral. For the particular case of the FRET couple YFP–CFP in an aqueous media $n = 1.4$, $Q_d = 0.42$ and $J = 1.4618e^{-13}$.

computationally accessible alternative to describe the trajectory of large conformational transitions in biomolecular systems. A similar methodology has proved its value in the improvement of a cAMP sensor characterizing the conformational behavior of short peptides used to link fluorescent modules fused to the two components of the Protein Kinase A (PKA) holoenzime [7]. In this contribution the description of an entire molecular probe is addressed. Simulations of the FRET sensor with two fluorescent modules fused to a cAMP-binding domain (Fig. 2) suggest that although orientational factors are not fully isotropic, they are highly dynamic making the inter-chromophore distance the dominant feature determining the functioning of the probes. It is expected that the use of *in silico* techniques may guide the rational design of new generations of fluorescent sensors for measuring intra cellular processes *in vivo*.

2. Methods

2.1. Comparison between explicit and implicit solvent simulations

The efficiency and reliability of the implicit solvation method was checked against the results of a previously published simulation of the isoform IIβ of the regulatory subunit of the PKA (PKARIIβ) [8]. The same coordinates used for the explicit solvent simulation of the free form of PKARIIβ were used as starting point for implicit solvation MD.

Simulations were performed using the generalized Born (GB) model for implicit solvation as implemented in Amber8 [9,10]. The standard implementation [11] and parameters [12] were used (option igb = 1 in the sander module of the Amber package). Given the potential impact of the different set of parameters used [13], test calculations were performed using the igb flag equal to 5, which corresponds to a different implementation and parameters for the effective Born radii [14]. However, both provided qualitatively the same results for bound and unbound probes. Notice however, that due to the looseness of the cAMP unbound state (see below), a rigorous comparison at the atomic level was not performed.

A cutoff radius of 2 nm and the Amber94 parameterization were adopted. The SHAKE method [15] was used to constrain all the bonded interactions after energy minimization. A thermalization period of 100 ps was adopted, in which the systems were heated up from 0 to 300 K. Trajectories for this simulation were collected for 1 ns recording one snapshot every 2 ps and used for analysis.

2.2. Choice of a FRET sensor

Among the vast variety of sensors existing in the literature, this work is focused on the probe reported in reference [16] called PKA-camps, which is based on the fluorescent couple CFP–YFP fused to the cAMP-binding domain B of RPKAIIβ. The rationale for this choice is the small size of this protein domain and the knowledge obtained from a previously reported MD based study on this isoform [8] containing both cAMP-binding domains. The results of this published simulation performed in the presence of explicit solvent can be used to check the reliability of the results presented here using the implicit solvent formalism. Furthermore, this class of proteins present a high structural conservation and similar conformational behavior among cAMP-binding domains [17–19], suggesting that all this homologous protein modules behave in a very similar fashion.

2.2.1. Structural models

The starting coordinates of the models were constructed using the segment from residues 264 to 403 of RPKAIIβ (PDB entry code: 1CX4 [20]) and two copies of the yellow spectral variant of GFP (YFP, PDB entry code: 1YFP [21] attached at the N and C termini of the cAMP-binding domain. This simplification is justified since YFP

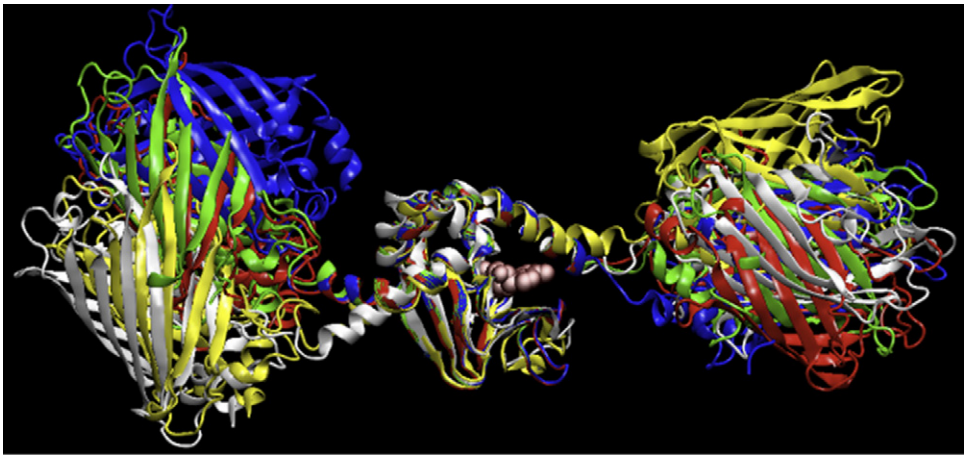

Fig. 2. Starting conformations for the simulated systems. Cartoon representation of the five initial conformers used for MD simulations. The cAMP bound probes were simulated with a molecule of cAMP (space fill, light red) within its binding domain. This molecule was removed for the cAMP free simulations.

and its fluorescent partner Cyan FP (CFP) are 97.4% identical with only two out of eight non-identical residues ($Ile146_{YFP} \rightarrow Asn_{CFP}$ and $Thr153_{YFP} \rightarrow Tyr_{CFP}$) pointing to the exterior of the β-can constituted by the fluorescent module. The chromophore within YFP was parameterized using the antechamber module of Amber8, while the parameters of cAMP were those reported by Punta et al. [22]. Since the relative orientation of the three protein modules was fixed arbitrarily, five independent simulations using different initial positions of the fluorescent modules with respect to the cAMP-binding domain were carried out and compared to enhance the conformational sampling (Fig. 2). A total of ten simulations lasting 10 ns each were performed (five for cAMP bound and five for free states) in order to obtain a description of the bound and free states [8,19].

The FRET efficiency for each single probe was calculated using the expression of Fig. 1. Interchromophore distance was measured from the centre of mass of each chromophore and the transition dipole moment of the chromophores was considered as the axis defined by the atoms C5 of the imidazole and C3 of the 4-oxo-benzene rings, respectively, according to the orientation for the transition dipole moment reported in reference [23].

Structural superposition of different isoforms of regulatory subunits of PKA was performed with MultiSeq [24] as implemented in VMD 1.8.5 [25].

3. Results

3.1. Implicit vs. explicit solvent simulations: The case of free PKARIIβ

The use of explicit representation for the solvent molecules in MD simulation is usually required to accurately consider the solvation effects (hydrophobic, electrostatic screening, etc.). However, for properly solvated systems, nearly 80% of the atoms in the computational box are solvent molecules, leading to a considerable increase of the computational cost. A much cheaper alternative is to consider implicitly the solvent as a continuum dielectric as, for example, the so called the generalized Born (GB) model scheme [12]. This has several advantages as lower computational cost, instantaneous dielectric response, no need of periodic boundaries. Moreover, the lack of viscosity related with the explicit water environment allows the system to more quickly and capably explore the available conformational space although faking the temporal scale of simulations. In fact, using GB simulations, an A-form DNA filament converges to its optimal B-form conformation nearly 25 times faster than in explicit water simulations [12].

Aimed to test the reliability of this simulation scheme to describe the cAMP driven allosteric mechanism of this protein system, a simulation of the β isoform of the regulatory subunit of the Protein Kinase A (PKARIIβ) was performed in this work using GB implicit solvation and compared with the results of explicit solvation simulations reported previously [8]. In this previous study in presence of explicit solvent, the removal of cAMP from the binding sites of PKARIIβ translates in a conformational transition. Briefly, PKARIIβ is constituted by two in-tandem cAMP-binding domains termed A and B. The absence of the ligands drives the protein to a more flexible state in which the C-terminal α-helices (C helices) of the cAMP-binding domains break at nearly 16 ns of MD simulation in presence of explicit solvent. Thus, the movement is transmitted to the rest of the protein [26,27] ultimately resulting in a conformational transition that separates the two cAMP-binding domains. This causes an increase of the average maximum linear dimension of about 1 nm and a reduction of the helical content of the whole protein [8]. Qualitatively, the same behavior was recovered during the implicit solvent simulation. Two main differences were found between the conformers obtained by explicit and implicit solvation simulations:

(i) Using explicit solvation, the binding domains A and B separate one from the other and the C helix of binding domain A remained in a flexible state, while using implicit solvation, besides the separation of both binding domains, the C-helix adopt a fully extended long helical segment (Fig. 3) sampling very similar conformations to those reported by Kim et al. PDB: 2qcs [28] and Wu et al. PDB: 2qvs [29] for the highly homologous isoforms of cAMP free PKARIα and PKARIIα in presence of the catalytic subunit. In close similarity with the PKARIα and PKARIIα structures, soon after the conformational transition a stiff salt bridge interaction between Glu282 and Arg381 was established (corresponding to those between Glu261, Arg366 and Glu265, Arg376 in PKARIα and PKARIIα, respectively). This suggests that in its free state the regulatory subunit of PKA adopts very similar conformations to that bound to its catalytic partner.

This leads to the conclusion that, despite the relatively large size of the system studied, the implicit solvation method provides a very reliable description of the allosteric transition in this class of proteins.

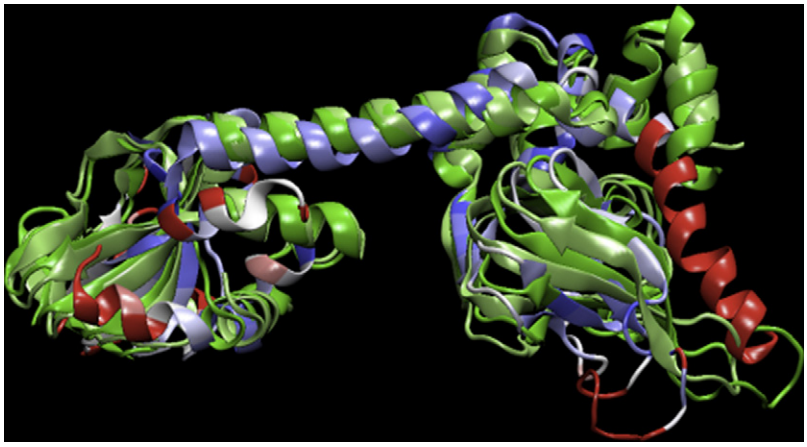

Fig. 3. Structural alignment of simulated and X-ray structures of PKAR isoforms. Superposition was performed between the MD conformer of PKARIIβ in its free state displaying the lowest RMSD with the X-ray structures of its isoforms PKARIα (green) and PKAIIα (light green). The model of PKARIIβ is colored by the RMSD of each residue with red (blue) for the worst (best) superimposing residues. The regions of worst superposition correspond to the N- and C-termini.

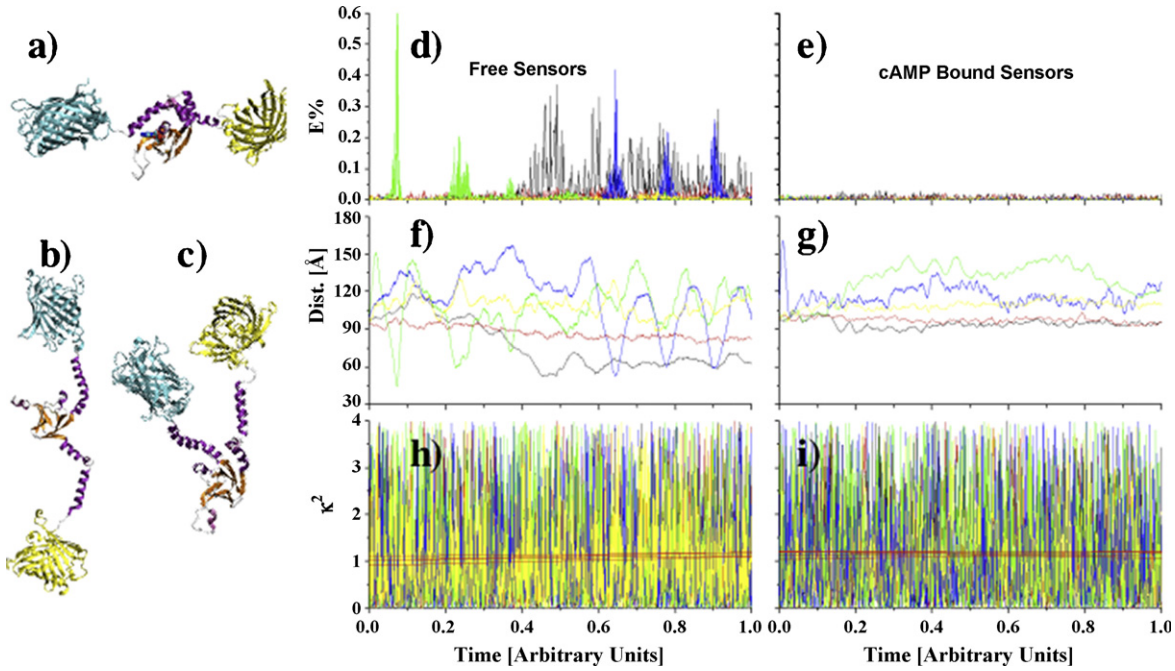

Fig. 4. Dynamical behavior of FRET sensor for cAMP. (a) Representative snapshot of a cAMP bound sensor during the dynamics. Both fluorescent modules remain at a minimal distance of nearly 9 nm, severely impairing the FRET. (b and c) Two typical conformers of cAMP free sensors. While the configuration shown in (b) keeps both fluorescent molecules far apart, the configuration in (c) highly favors FRET. (d and e) The simulated FRET efficiency for cAMP free and bound, respectively. Different colors indicate independent simulations. Notice the correlation between the peaks in FRET efficiency with the minima in the interchromophore distances shown in (f) for the free sensors. In contrast, the interchromophore distances for the cAMP bound proves (g) show a more monotonous behavior with distances above 9 nm. (h and i) Orientational factors for free and bound sensors, respectively. They sample evenly the whole range of values between 0 and 4 regardless the case. Nearly horizontal red lines suggest a sable and well converged behavior.

(ii) The second important difference regards the temporal scale. While the detachment of both cAMP-binding domains in the explicit solvation case took about 16 ns, the same process took less than 400 ps in the implicit solvent simulation. This large difference in mobility is likely attributable to the lack of viscosity in the latter case and indicates a speed up in the sampling time of nearly two orders of magnitude. Although this represents an advantage for the conformational sampling, GB is clearly unable to properly describe the temporal scale since it remains intimately related to the intrinsic viscosity of each molecule. Therefore, the time scales in Fig. 4 are reported in arbitrary units to underline this fact.

Having assessed the reliability of the GB framework for describing the cAMP driven allosteric mechanism, the more challenging case of the FRET sensors for measuring cAMP concentrations *in vivo* was addressed.

Grossly, the MD trajectories of the probes resulting from simulations using different starting conformations (Fig. 2) show qualitatively similar results, suggesting that the conformational sampling achieved is reasonably large enough to get a representative picture of the dynamical behavior of the probes. Therefore, the description of the results henceforward will be regarded to the "free" and "bound" systems as representatives of two different states.

In the cAMP bound state, the presence of the ligand stabilizes the structure of the binding site and their folding is well maintained. This keeps both fluorescent modules far apart from each other (Fig. 4a) with a minimum interchromophore distance of 9 nm. Hampering the FRET effect and keeping the transfer efficiency to minimum values (Fig. 4d).

In the free state the cAMP-binding domains undergo a conformational change that is completely analogous to those already described above and in other published MD simulations of cAMP-binding domains in the presence of explicit solvent (namely, the full length RPKAIIβ [8]) and the cAMP-binding domain of the HCN2 channel [19]). However, a worth difference is observed between the previous explicit solvent simulations and those performed here using the GB method. While in the former the C helix displayed a large mobility, in the latter it completely detaches from the binding pocket leaving the structure of the β-roll substantially unaltered, reminiscent to the X-ray structure of the EPAC cAMP-binding module in its free state [26]. This conformational transition takes place between 100 ps and 400 ps using implicit solvent simulations in the five independent simulations presented in this work. Detachment of the C helix from the cAMP-binding pocket translates in a reduction of the distance between the N and C termini of the cAMP-binding domain, and hence, between the two fluorescent modules.

In this state both fluorescent modules are able to move with a pivotal point at their junction with the β-roll (Fig. 4b and c). So, they can eventually explore loose conformations in which they can be either closer of farther than in the cAMP bound state. This behavior translates in fluctuating interchromophore distances that eventually generate marked increases in the FRET signal (Fig. 4). Clearly, while considering the signal produced by one single probe results in discrete peaks, the global effect of the large number of fluorescent sensors in a cellular environment result in homogeneous light spots localized in space and time.

The peaks observed in the FRET efficiency signal display a finer modulation due to the faster behavior of the orientational (κ^2) factor, i.e., while the interchromophore distance varies slowly because it is linked to a conformational change in the cAMP-binding domain, κ^2 varies with the relative orientation between chromophores that can change due to the rotation of a single sigma bond along segments of unstructured protein backbone that link

the fluorescent modules to the cAMP-binding domains. The time dependency of κ^2 (Fig. 4h and i) shows a rather homogeneous distribution of the possible values between 0 and 4. A linear fit over the simulated time gives nearly horizontal lines with almost identical Y-intercept values of 1.1 and 1.05 for a the bound and free probes, respectively, averaged over the five simulated conformers. This result is in contrast with the usually assumed 2/3 value (isotropic hypothesis).

This data indicates that the FRET efficiency in this kind of probes depends essentially on the interchromophore distance while the orientational factors have little relevance. Furthermore, while the common intuition suggests two distinct conformations corresponding to FRET/no-FRET states, only the cAMP bound (no-FRET) state is well defined (Fig. 4). In absence of cAMP both fluorescent modules can move freely exploring conformations that may or may not be favorable for FRET.

4. Conclusions

The results of the simulations presented in this contribution constitute the first attempt to describe the molecular mechanism of genetically encoded fluorescent sensor for monitoring intracellular events *in vivo* using theoretical tools. The description achieved through the use of implicit solvation MD simulations captures the essential features of this kind of probes. This computer-aided methodology may be generally applied to different systems in which allosteric transitions may be described by MD techniques to establish new time-saving design strategies for biomedical research.

Acknowledgment

This work has been performed thanks to supercomputer time granted by CNISM–CINECA. I thank Alejandro Pantano for useful discussions.

Reference

[1] T. Förster, Ann. Physiol. 2 (1948) 55–75.
[2] R. Rudolf, M. Mongillo, R. Rizzuto, T. Pozzan, Looking forward to seeing calcium, Nat. Rev. Mol. Cell Biol. 4 (2003) 579–586.
[3] M. Zaccolo, P. Magalhaes, T. Pozzan, Compartmentalisation of cAMP and Ca(2+) signals, Curr. Opin. Cell Biol. 14 (2002) 160–166.
[4] M. Zaccolo, Use of chimeric fluorescent proteins and fluorescence resonance energy transfer to monitor cellular responses, Circ. Res. 94 (2004) 866–873.
[5] J.R. Lakowicz, Energy transfer, in: Principles of Fluorescence Spectroscopy, Plenum, New York, 2006, pp. 443–452.
[6] J. Zhang, R.E. Campbell, A.Y. Ting, R.Y. Tsien, Creating new fluorescent probes for cell biology, Nat. Rev. Mol. Cell Biol. 3 (2002) 906–918.
[7] V. Lissandron, A. Terrin, M. Collini, L. D'alfonso, G. Chirico, S. Pantano, M. Zaccolo, Improvement of a FRET-based indicator for cAMP by linker design and stabilization of donor–acceptor interaction, J. Mol. Biol. 354 (2005) 546–555.
[8] S. Pantano, M. Zaccolo, P. Carloni, Molecular basis of the allosteric mechanism of cAMP in the regulatory PKA subunit, FEBS Lett. 579 (2005) 2679–2685.
[9] W.D. Cornell, P. Cieplak, C.I. Bayly, I.R. Gould, K.M. Merz, D.M. Ferguson, D.C. Spellmayer, T. Fox, J.W. Caldwell, P.A. Kollman, A second generation force field for the simulation of proteins, nucleic acids, and organic molecules, J. Am. Chem. Soc. 117 (1995) 5179–5197.
[10] D.A. Case, T.A. Darden, T.E. Cheatham III, C.L. Simmerling, J. Wang, R.E. Duke, R. Lou, K.M. Merz, B. Wang, D.A. Pearlman, M. Crowley, S. Brozell, V. Tsui, H. Gohlke, J. Mongan, V. Hornak, G. Cui, P. Beroza, C. Schafmeister, J.W. Caldwell, W.S. Ross, P.A. Kollman, Amber 8.0, University of California, San Francisco, California, 2004 .
[11] G.D. Hawkins, C.J. Cramer, D.G. Truhlar, Parameterized models of aqueous free energies of solvation based on pairwise descreening of solute atomic charges from a dielectric medium, J. Phys. Chem. 100 (1996) 19824–19839.
[12] V. Tsui, D.A. Case, Theory and applications of the generalized Born solvation model in macromolecular simulations, Biopolymers 56 (2000) 275–291.
[13] A. Onufriev, D.A. Case, D. Bashford, Effective Born radii in the generalized Born approximation: the importance of being perfect, J. Comput. Chem. 23 (2002) 1297–1304.
[14] A. Onufriev, D. Bashford, D.A. Case, Exploring protein native states and large-scale conformational changes with a modified generalized born model, Proteins 55 (2004) 383–394.
[15] J.P. Ryckaert, G. Ciccotti, H.J. Berendsen, Numerical integration of the Cartesian equations of motion of a system with constraints: molecular dynamics of *n*-Alkanes, J. Comput. Phys. 23 (1977) 327–341.
[16] V.O. Nikolaev, M. Bunemann, L. Hein, A. Hannawacker, M.J. Lohse, Novel single chain cAMP sensors for receptor-induced signal propagation, J. Biol. Chem. 279 (2004) 37215–37218.
[17] H.M. Berman, L.F. Ten Eyck, D.S. Goodsell, N.M. Haste, A. Kornev, S.S. Taylor, The cAMP binding domain: an ancient signaling module, Proc. Natl. Acad. Sci. U.S.A. 102 (2005) 45–50.
[18] M. Berrera, S. Pantano, P. Carloni, Catabolite activator protein in aqueous solution: a molecular simulation study, J. Phys. Chem. B 111 (2007) 1496–1501.
[19] M. Berrera, S. Pantano, P. Carloni, cAMP Modulation of the cytoplasmic domain in the HCN2 channel investigated by molecular simulations, Biophys. J. 90 (2006) 3428–3433.
[20] T.C. Diller, N.H. Madhusudan, S.S. Xuong, Taylor, Molecular basis for regulatory subunit diversity in cAMP-dependent protein kinase: crystal structure of the type II beta regulatory subunit, Structure 9 (2001) 73–82.
[21] R.M. Wachter, M.A. Elsliger, K. Kallio, G.T. Hanson, S.J. Remington, Structural basis of spectral shifts in the yellow-emission variants of green fluorescent protein, Structure 6 (1998) 1267–1277.
[22] M. Punta, A. Cavalli, V. Torre, P. Carloni, Molecular modeling studies on CNG channel from bovine retinal rod: a structural model of the cyclic nucleotide-binding domain, Proteins 52 (2003) 332–338.
[23] F.I. Rosell, S.G. Boxer, Polarized absorption spectra of green fluorescent protein single crystals: transition dipole moment directions, Biochemistry 42 (2003) 177–183.
[24] E. Roberts, J. Eargle, D. Wright, Z. Luthey-Schulten, MultiSeq: unifying sequence and structure data for evolutionary analysis, BMC Bioinformatics 7 (2006) 382.
[25] W. Humphrey, A. Dalke, K. Schulten, VMD: visual molecular dynamics, J. Mol. Graph. 14 (1996) 33–38.
[26] H. Rehmann, B. Prakash, E. Wolf, A. Rueppel, J. de Rooij, J.L. Bos, A. Wittinghofer, Structure and regulation of the cAMP-binding domains of Epac2, Nat. Struct. Biol. 10 (2003) 26–32.
[27] G.M. Clayton, W.R. Silverman, L. Heginbotham, J.H. Morais-Cabral, Structural basis of ligand activation in a cyclic nucleotide regulated potassium channel, Cell 119 (2004) 615–627.
[28] C. Kim, C.Y. Cheng, S.A. Saldanha, S.S. Taylor, PKA-I holoenzyme structure reveals a mechanism for cAMP-dependent activation, Cell 130 (2007) 1032–1043.
[29] J. Wu, S.H. Brown, S. von Daake, S.S. Taylor, PKA type IIalpha holoenzyme reveals a combinatorial strategy for isoform diversity, Science 318 (2007) 274–279.